Article

Energy and Economic Assessment of Energy Efficiency Options for Energy Districts: Case Studies in Italy and Egypt

Francesco Calise [1], Francesco L. Cappiello [1,*], Maria Vicidomini [1], Jian Song [2], Antonio M. Pantaleo [2,3], Suzan Abdelhady [4], Ahmed Shaban [5] and Christos N. Markides [2]

1   Department of Industrial Engineering, University of Naples Federico II, P.le Tecchio 80, 80125 Naples, Italy; frcalise@unina.it (F.C.); maria.vicidomini@unina.it (M.V.)
2   Clean Energy Processes Laboratory, Imperial College London, London SW7 2AZ, UK; jian.song@imperial.ac.uk (J.S.); antonio.pantaleo@uniba.it (A.M.P.); c.markides@imperial.ac.uk (C.N.M.)
3   Department of Agriculture and Environmental Sciences, University of Bari, Via Amendola 165/A, 70125 Bari, Italy
4   Electrical Engineering Department, Faculty of Engineering, Fayoum University, 63514 Fayoum, Egypt; suzan.abdelhady@fayoum.edu.eg
5   Mechanical Engineering Department, Faculty of Engineering, Fayoum University, 63514 Fayoum, Egypt; ahmed.shaban@fayoum.edu.eg
*   Correspondence: francescoliberato.cappiello@unina.it

Abstract: In this research, a technoeconomic comparison of energy efficiency options for energy districts located in different climatic areas (Naples, Italy and Fayoum, Egypt) is presented. A dynamic simulation model based on TRNSYS is developed to evaluate the different energy efficiency options, which includes different buildings of conceived districts. The TRNSYS model is integrated with the plug-in Google SketchUp TRNSYS3d to estimate the thermal load of the buildings and the temporal variation. The model considers the unsteady state energy balance and includes all the features of the building's envelope. For the considered climatic zones and for the different energy efficiency measures, primary energy savings, pay back periods and reduced CO_2 emissions are evaluated. The proposed energy efficiency options include a district heating system for hot water supply, air-to-air conventional heat pumps for both cooling and space heating of the buildings and the integration of photovoltaic and solar thermal systems. The energy actions are compared to baseline scenarios, where the hot water and space heating demand is satisfied by conventional natural gas boilers, the cooling demand is met by conventional air-to-air vapor compression heat pumps and the electric energy demand is satisfied by the power grid. The simulation results provide valuable guidance for selecting the optimal designs and system configurations, as well as suggest guidelines to policymakers to define decarbonization targets in different scenarios. The scenario of Fayoum offers a savings of 67% in primary energy, but the associated payback period extends to 23 years due to the lower cost of energy in comparison to Naples.

Keywords: space heating; space cooling; energy efficiency; renewable energy; energy and economic assessment

1. Introduction

The EU has ambitious climate goals that target reducing greenhouse gas (GHG) emissions by 50% relative to the current levels by 2030, a rise of renewable energy sources to 27% and an overall growth of energy efficiency measures of 27%. The long-term target is to abate GHG emissions by 80–95% relative to the 1990 levels by 2050. These goals require a massive adoption of renewable energy sources (RES) technologies and the implementation of high-efficiency energy measures. Energy demands in residential buildings contribute with a large share of the total demand [1]. Accordingly, both the reduction of primary energy consumption and the mitigation of local emissions in residential sectors necessitates a portfolio of technologies as proposed in the literature, such as district heating and

cooling networks (DHC) [2,3]. DHC is particularly promising for low-temperature heat, which could be produced by solar energy [4,5], geothermal energy [6,7] and/or by waste heat recovery [8,9], and the system integration of these technologies to provide flexibility and sector coupling functionalities is particularly promising [10,11]. In this context, heat pumps (HPs) appear as an interesting option; could operate at various temperature levels according to the selected technology, working fluid and system integration level and could be coupled to photovoltaic (PV) systems and DH networks to match the residential energy demand [12,13]. Several simulation tools are available in the literature, spanning from single building-level tools such as Energy-Plus and TRNSYS, focused on high temporal resolution and time horizons from seconds to weeks, to district or national-level analyses such as Energy-PLAN and enlarging the focus to a broader integration of water, industry, transport sectors and other sector coupling possibilities.

The hybridization of solar thermal collectors (STC) and photovoltaic (PV) are broadly implemented as renewable energy solutions for domestic sectors. For hot water and space heating, both evacuated tube collectors (ETC) and flat plate collectors (FPC) are adopted. In the plant of solar-HP hybrid technologies for buildings, a solar system for heating and cooling, based on a PV combined to an HP was proposed to match the energy demand of an office in Southern Italy [14]. Dynamic simulations were performed to analyze the energy, environment and economics at different technical and economical parameters that included the tilt angle, peak power of PV, electricity price and natural gas price. This option based on solar energy integration reported a primary energy savings of 81% due the reduction of fossil fuel consumption and equivalent CO_2 emission when compared to a conventional natural gas boiler and an electric-driven chiller. In addition, the same research [14] compared the performance of solar thermal and solar electrical cooling systems in two different European countries (Germany and Spain) for a residential building, reporting an expected primary energy savings of up to 40% for Germany's building and up to 60% for Spain's building both for the STC collectors and PV modules. To fulfill the demand of an office building for space heating and cooling, a PV-driven heat pump equipped with a battery storage system was considered in Reference [15], analyzing the thermo-economic performances at different peak powers of PV and the battery capacity by means of TRNSYS.

A promising solution proposed in [16] for buildings considers carbon dioxide (CO_2) HPs in comparison to conventional systems to produce hot water with large temperature lifts in comparison to conventional air-to-air heat pumps, particularly when the water temperature is higher than 60 °C, as also reported in Reference [16]. Although CO_2 vapor compression heat pumps are widely adopted in heating/cooling applications, the high temperature of the discharge and return from the consumer significantly reduce the performance. Previous studies have addressed the performance of CO_2 HP-based hot water production systems, considering both experimental and numerical approaches [16,17].

Other interesting approaches for energy systems optimization in building sectors to investigate the influence of energy models and indoor air quality are also available in the literature [18].

However, the combination and integration of HP and PV technologies in residential sectors have not been widely investigated, and the research has been mostly focused on the single building-level [19], with limited focus on district-scale applications [20]. In this research, the energy and economic evaluations of some promising integration of renewable energy technologies and energy efficiency measures at the district level are performed using a novel transient simulation tool. In particular, this work compares PV modules and ETCs solar options, coupled to air-to-air conventional HP/chillers, for the areas of Naples (South of Italy) and Fayoum (Egypt).

The main novelties of this work are summarized as follows.

- This paper analyzes the energy, environmental and economic performances of several energy measures for two districts with different climate—namely, cold paint adoption, boiler replacement and a renewable option based on the evacuated solar collector.

- The analysis of the energy performance of cold paint for a high-irradiance country (Egypt), highlighting how the solar gain affects the district energy demand.
- The comparison of the performance of the renewable energy options in Naples and Fayoum, highlighting the potentials for reducing the environmental impact of residential districts.
- The present work is able to provide a green pathway for achieving a sustainable residential district with a very low primary energy consumption.

The paper is organized as follows. The system layout and configuration are presented in Section 2, and the related system models based on TRNSYS are presented in Section 3. The case study and the related results are provided Sections 4 and 5. The conclusions and future work directions are outlined in Section 6.

2. System Layout

This research proposes an innovative system that includes a district heating network that can provide hot water and space heating; the space heating demand is met by air-to-air heat pumps coupled to a district PV plant. The district heating network is fed by an ETC plant, as shown in Figure 1. Moreover, the PV plant satisfies a share of the electricity demand.
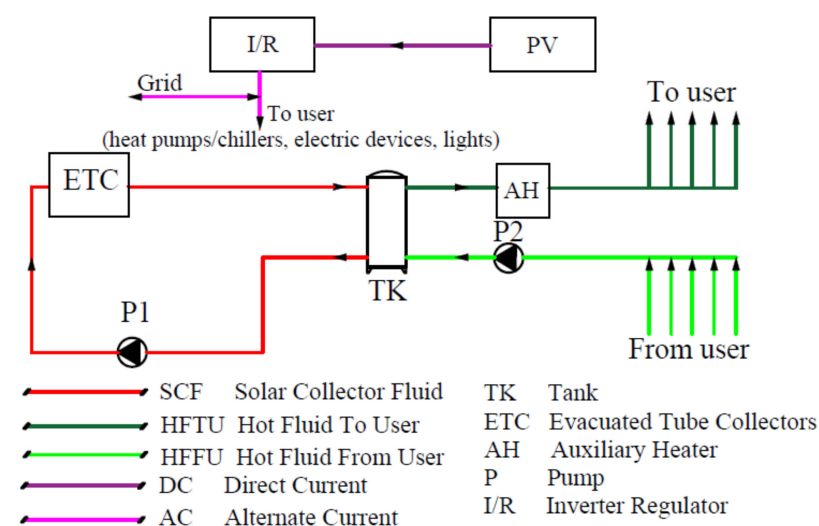

Figure 1. Proposed system layout for the districts in Italy and Egypt.

The electric energy demand of the district is formed by: (i) the electrical appliances installed in the buildings, (ii) the lighting equipment and (iii) the space heating and cooling by electric-driven heat pumps for (iv) the hydraulic auxiliary system for domestic hot water provision from the district heating network (DHDWH) (Figure 1).

The PV plant and ETC plant capacities are calculated to maximize the self-consumed renewable energy.

The proposed layout consists of two main thermal loops (Figure 1). The Solar Collector Fluid loop (SCFL) is based on water heated by the ETCs and supplied to the solar tank (TK). A feedback controller is included to control the variable speed pump "P1" (Figure 1), which enables the ETC outlet temperature to reach the set value by varying the pump flow rate. $T_{set,ETC}$, as reported in Table 1, is set at 50 °C for Naples and Fayoum (Figure 1). The controller is designed to turn off the pump "P1" when the temperature of the ETC outlet is lower than the temperature of the tank outlet, preventing the heat dissipation when the solar radiation is not sufficient.

Table 1. The design and operating parameters of the system components. ETC: evacuated tube collectors and PV: photovoltaic.

Component	Parameter	Description	Value	Unit
ETC	a_1	First order efficiency coefficient	2.78	$Wm^{-2}K^{-1}$
	a_2	Second order efficiency coefficient	0.0083	$Wm^{-2}K^{-2}$
	A_{ETC} (*Naples*)	Aperture area of solar collector for Naples	1700	m^2
	A_{ETC} (*Fayoum*)	Aperture area of solar collector for Fayoum	1700	m^2
	q_{P2}	Rated flow rate of PSol	85,000	kg/h
	η_0	SC Zero loss efficiency at normal incidence	0.70	-
	cp	Specific heat of water	4.190	kJ/kg K
	α	Collector Slope	30	$^\circ$
	β	Collector Azimuth	0	
	$T_{set,ETC}$ (*Naples*)	SC outlet set point temperature for Naples proposed system	50	$^\circ C$
	$T_{set,ETC}$ (*Fayoum*)	SC outlet set point temperature for Fayoum proposed system	50	
	$T_{set,tUsers}$	Set point temperature for Users	54	
PV	P_{max}	Maximum PV power	260	W_P
	V_{oc}	Voltage of open-circuit	37.7	V
	I_{sc}	Current of short-circuit	9.01	A
	V_{mpp}	Voltage at MPP	30.5	V
	I_{mpp}	Current at MPP	8.51	A
	N_s	Number of modules in series	2	-
	N_p (*Naples*)	Number of modules in parallel for Naples	2920	
	N_p (*Fayoum*)	Number of modules in parallel for Fayoum	2920	
	A	PV module area	1.6	m^2
	N_{cell}	Number of PV cells in series	15	-
	η_{PV}	Efficiency of PV module	15.8	
	$P_{rated,PV}$	Rated power of PV panel	570	kW
	A_{tot} (*Naples*)	PV plant area	9397	m^2
	A_{tot} (*Fayoum*)	PV plant area	9397	m^2

The district heating domestic hot water network (DH-DHW-N) supplies the DHW to residential buildings. The mass flow rate of this network is controlled by the variable speed pumps (P_{h-i}, i = A, B, C and D). A feedback controller handles each pump P_{h-I}, and the controller is designed to meet the user's demand for the thermal flow rate by employing the minimum water flow rate. The adoption of such an approach is able to reduce the pumping power consumption and to enhance the energy performance of the district network [21,22].

A gas-fired condensing boiler (CB) is installed, as a backup system, to keep the temperature of the flow delivered to the users above the assumed set point temperature $T_{set,forUser}$ (54 $^\circ C$ for both locations).

The PV plant is sized to fulfill a share of the electricity demand. When the PV plant output is lower than the demand, the remaining amount of electricity demand is withdrawn from the power grid. Moreover, if the PV plant output exceeds the demand, the excess output is delivered/sold to the grid. Therefore, it is assumed that there is no electricity storage system in this system.

3. System Models

The renewable energy system was modeled in TRNSYS, which offers high accuracy and reliability for dynamic simulations—in particular, for energy demand assessments [23]. A library with experimentally validated built-in components and technologies is included in TRNSYS [24], along with user-customized models. TRNSYS also allows the user to develop and integrate in-house models.

The components/technologies considered in this study are listed below:

- Type 56: This library takes the building's 3D geometry, the thermophysical proprieties of the envelope and the effects of the environment into account to dynamically evaluate the energy performance of the building. Reference [25] provides a detailed description of this library.
- Type 94: This library models the PV panel performance using the "*four parameters*" method [25].
- Type 71: This library simulates the ETC performance using the Hottel–Whillier–Bliss equation [26]. Reference [23] gives a detailed description of Type 71.

The geometrical model of the district buildings considered in this study was developed using the Google SketchUp TRNSYS3d plug-in [27] and is linked to the TRNSYS environment via Type 56, which allows the user to simulate the building's thermal performance.

Thermoeconomic Model

The primary energy consumption (PE) of the reference system (RS) considered for both districts, i.e., Naples and Fayoum, is evaluated as follows:

$$PE_{RS} = \sum_t \left[\left(E_{el,LOAD} + \frac{E_{th,cool}}{COP_n} \right) \frac{1}{\eta_{el}} + \left(\frac{E_{th,heat}}{\eta_B} + \frac{E_{th,DHW}}{\eta_B} \right) \right]_t \tag{1}$$

where COP_n represents the coefficient of performance of the heat pumps, $E_{el,LOAD}$ is the total electricity demand, η_{el} is the efficiency of the conventional power plants (Table 2), η_B is the efficiency of the conventional-fired boilers (Table 2) and $E_{th,heat}$ and $E_{th,cool}$ are the annual heating and cooling demand for the heating and cooling of the space.

Note that the COP is dynamically evaluated according to the equations provided in Reference [25].

The *PE* of the proposed systems (PS) are evaluated employing the following equations:

$$PE_{PS1} = \sum_t \left[\left(E_{el,LOAD} + \frac{E_{th,cool}}{COP_n} + \frac{E_{th,heat}}{COP_n} \right) \frac{1}{\eta_{el}} + \left(\frac{E_{th,DHW}}{\eta_B} \right) \right]_t$$

$$PE_{PS2} = \sum_t \left[\left(E_{el,LOAD} + \frac{E_{th,cool}}{COP_n} \right) \frac{1}{\eta_{el}} + \left(\frac{E_{th,heat}}{\eta_B} + \frac{E_{th,DHW}}{\eta_B} \right) \right]_t \tag{2}$$

$$PE_{PS3} = \sum_t \left[\left(E_{el,fromGRID} - E_{el,toGRID} \right) \frac{1}{\eta_{el}} + \left(\frac{E_{th,DHW,aux}}{\eta_{CB}} \right) \right]_t$$

where η_{CB} denotes the efficiency of the conventional and condensing gas-fired boilers (Table 2), and $E_{th,DHW,aux}$ represents the thermal energy provided by the auxiliary condensing boiler, when the thermal energy generated by ETCs is not enough to fulfill the total heating demand of the district.

Note that the following energy measures have been considered:

k = 1: refers to the layout with thermophysical properties improvement for the building envelope, and

k = 2: refers to the renewable energy layout described in Section 2 System Layout.

The primary energy saving for the PS is calculated as follows:

$$\Delta PE_{PSk} = PE_{RS} - PE_{PSk}$$

$$PES_{PSk} = \frac{PE_{RS} - PE_{PSk}}{PE_{RS}} \tag{3}$$

The yearly operating costs (*C*) of the RS are evaluated according to Equation (4).

$$C_{RS} = \sum_t \left[\left(E_{el,LOAD} + \frac{E_{th,cool}}{COP_n} \right) J_{el,fromGRID} + \left(\frac{(E_{th,heat} + E_{th,DHW})/\eta_B}{LCV_{NG}} \right) J_{NG} \right]_t \qquad (4)$$

The yearly operating costs of the proposed systems are evaluated as follows:

$$
\begin{aligned}
C_{PS1} &= \sum_t \left[\left(E_{el,LOAD} + \frac{E_{th,cool}}{COP_n} \right) J_{el,fromGRID} + \left(\frac{(E_{th,heat} + E_{th,DHW})/\eta_B}{LCV_{NG}} \right) J_{NG} \right]_t \\
C_{PS2} &= \sum_t \left[\left(E_{el,LOAD} + \frac{E_{th,cool}}{COP_n} + \frac{E_{th,heat}}{COP_n} \right) J_{el,fromGRID} + \left(\frac{(E_{th,DHW})/\eta_B}{LCV_{NG}} \right) J_{NG} \right]_t \\
C_{PS3} &= \sum_t \left[E_{el,fromGRID} J_{el,fromGRID} - E_{el,toGRID} J_{el,toGRID} + \left(\frac{(E_{th,DHW,aux})/\eta_{CB}}{LCV_{NG}} \right) J_{NG} + m_{PV} + m_{ETC} \right]_t
\end{aligned}
\qquad (5)$$

where $J_{el,fromGRID}$ and $J_{el,toGRID}$ are the purchasing and the selling price of electricity from/to the grid, respectively, J_{NG} is the natural gas cost and m_{ETC} and m_{PV} denote the costs of the annual maintenance for the ETC and PV plant (Table 2).

The annual savings are calculated as follows:

$$\Delta C_{PSk} = \frac{C_{RS} - C_{PSk}}{C_{RS}} \qquad (6)$$

The capital cost (*C*$_{inv}$) for the two different energy measures is evaluated with the following equations:

$$
\begin{aligned}
C_{inv,PS1,Fayoum} &= C_{CP,roof} + C_{CP,wall} \\
C_{inv,PS2,Fayoum} &= 0 \\
C_{inv,PS3,Fayoum} &= C_{CB,aux} + C_{PV} + C_{ETC} + C_{pumps} + C_{TK} + C_{piping}
\end{aligned}
\qquad (7)$$

Two different types of building envelope energy measures were considered for the two selected locations based on the typical features of each weather zone, which will be clarified in the Section 4 Case Study.

Table 2 displays the terms used in these equations. Note that the district installation cost is evaluated according to References [28,29].

The Profit Index (*PI*), net present value (*NPV*) and simple payback period (*SPB*) are given by:

$$
\begin{aligned}
SPB_{PSk} &= \frac{C_{inv,k}}{\Delta C_{PS}} \\
PI_{PSk} &= \frac{\Delta C_{PS} \cdot AF - C_{inv,PSk}}{C_{inv,PSk}} \\
NPV_{PSk} &= PI_{PSk} C_{inv,PSk}
\end{aligned}
\qquad (8)$$

where *AF* is the annuity factor, which is considered as 14.09 years, assuming a time horizon of 25 years.

The environmental performance is evaluated by employing the following equations:

$$
\begin{aligned}
CO_{2,PS1} &= \sum_t \left[\left(E_{el,LOAD} + \frac{E_{th,cool}}{COP_n} \right) F_{el} + \left(\frac{E_{th,heat}}{\eta_B} + \frac{E_{th,DHW}}{\eta_B} \right) F_{NG} \right]_t \\
CO_{2,PS2} &= \sum_t \left[\left(E_{el,LOAD} + \frac{E_{th,cool}}{COP_n} + \frac{E_{th,heat}}{COP_n} \right) F_{el} + \left(\frac{E_{th,DHW}}{\eta_B} \right) F_{NG} \right]_t \\
CO_{2,PS3} &= \sum_t \left[\left(E_{el,fromGRID} - E_{el,toGRID} \right) F_{el} + \left(\frac{E_{th,DHW,aux}}{\eta_{CB}} \right) F_{NG} \right]_t \\
\Delta CO_{2,PSk} &= \frac{CO_{2,RSk} - CO_{2,PSk}}{CO_{2,RS}}
\end{aligned}
\qquad (9)$$

Table 2 lists the terms adopted in this equation.

<div align="center">**Table 2.** Thermo-economic and environmental data.</div>

Parameter		Description	Value (Unit)
$C_{windows}$		Replacement cost of windows per m^2	300 (€/m^2)
C_{CP}		Cool paint cost per m^2	2.91 (€/m^2) [30]
$C_{CB,aux}$		Cost of auxiliary condensing boiler	40 (€/kW$_{th}$)
C_{ETC}		Capital cost of ETC unit per m^2 of solar plant	300 (€/m^2) [5]
C_{PV}		Capital cost of PV unit per kW$_{el}$	1000 (€/kW$_{el}$) [31]
C_{TK}		The tank cost	$C_{TK} = 494.9 + 808.0 \cdot V_{TK}$ (€) [32]
C_{pumps}	*small*	The small pumps costs	$C_P = 1.08 \cdot (-2 \cdot 10^{-8} \cdot \dot{m}^2 + 0.0285 \cdot \dot{m} + 388.14)$ (€) [33]
	40 m^3/h	The Salmson pump cost (40 m^3/h)	1490 (€/pump) [34]
	80 m^3/h	The Salmson pump cost (80 m^3/h)	1900 [€/pump) [34]
C_{piping}		Piping cost for district heating network	33 (€/m) [28]
$J_{el,fromGRID}$ (*Naples*)		Purchasing price of electric energy	0.18 (€/kWh)
$J_{el,toGRID}$ (*Naples*)		Selling price electric energy	0.07 (€/kWh)
J_{NG} (*Naples*)		Purchasing price of natural gas	0.88 (€/Sm^3)
$J_{el,fromGRID}$ (*Fayoum*)		Purchasing price of electric energy	0.0764 (€/kWh)
$J_{el,toGRID}$ (*Fayoum*)		Selling price electric energy	0.07 (€/kWh)
J_{NG} (*Fayoum*)		Purchasing price of natural gas	0.1186 (€/Sm^3)
m_{ETC}		Annual maintenance cost ETC	2 (%/year)
m_{PV}		Annual maintenance cost for PV	1.5 (%/year)
LHV_{NG}		Lower heating value of natural gas	9.59 (kWh/Sm^3)
η_{el} (*Naples*)		Efficiency of conventional electric power plant	46 (%)
η_{el} (*Fayoum*)		Efficiency of conventional electric power plant	45.9 (%)
η_B		Efficiency of natural gas boiler	75 (%)
η_{CB}		Efficiency natural gas condensing boiler	95 (%)
F_{NG}		Equivalent CO$_2$ emissions coefficient for natural gas	0.20 (kgCO$_2$/kWh$_{PE}$)
F_{el} (*Naples*)		Equivalent CO$_2$ emissions coefficient for electricity in Naples	0.48 (kgCO$_2$/kWh$_{el}$)
F_{el} (*Fayoum*)		Equivalent CO$_2$ emissions coefficient for electricity in Fayoum	0.431 (kgCO$_2$/kWh$_{el}$)

4. Case Study

Two small residential districts (each with 50 buildings, as shown in Figure 2) located in Naples (Italy) and Fayoum (Egypt) are considered.

Figure 2. Building geometric 3D models.

The districts modeling approach is described in detail in Reference [35]. Four constructive types of buildings (Figure 2) are considered for the selected districts. These four geometrical types of buildings are coupled with three types of end users: families, young

people and old people. Table 3 summarizes the occupancy characteristics of the buildings. Considering the construction age of the selected buildings, the thermal insulation is assumed to be quite poor, with U set at 0.9–1.2 W/m^2 K (see Table 4) [22,36]. Due to the fact that the selected residential districts are very crowded (Figure 3), the building shading is also considered, as shown in Figure 4.

Table 3. Occupancy characteristics of the district buildings for Naples and Fayoum.

Building Type	Number of Buildings		
	Family	Old People	Young People
A (Naples)	9	3	2
B (Naples)	9	3	2
C (Naples)	8	3	-
D (Naples)	8	3	-
A (Fayoum)	9	2	2
B (Fayoum)	9	3	2
C (Fayoum)	9	3	-
D (Fayoum)	8	3	-

Table 4. Envelope features for each building.

| Building Element	Buildings A, B, C and D			
	U-Value (W/m^2 K)	Thickness (m)	ρ_s (–)	ε (–)
Roof (Naples)	0.916	0.255		
Façades (Naples)	1.204	0.240	0.4	0.9
Ground floor (Naples)	1.030	0.285		
Adjacent ceiling (Naples)	1.157	0.295		
Windows glass (Naples)	2.89	0.004/0.016/0.004	0.13	0.18
Roof (Fayoum)	1.377	0.155	0.4	0.9
Façades (Fayoum)	1.728	0.150		
Ground floor (Fayoum)	1.030	0.285		
Adjacent ceiling (Fayoum)	1.157	0.295		
Windows glass (Fayoum)	2.89	0.004/0.016/0.004	0.13	0.18
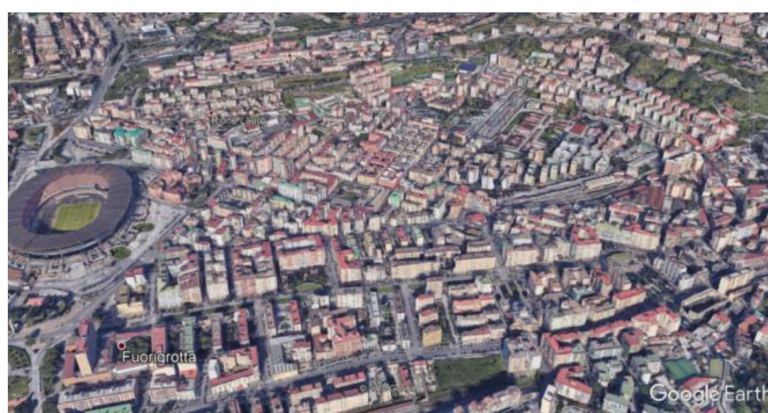
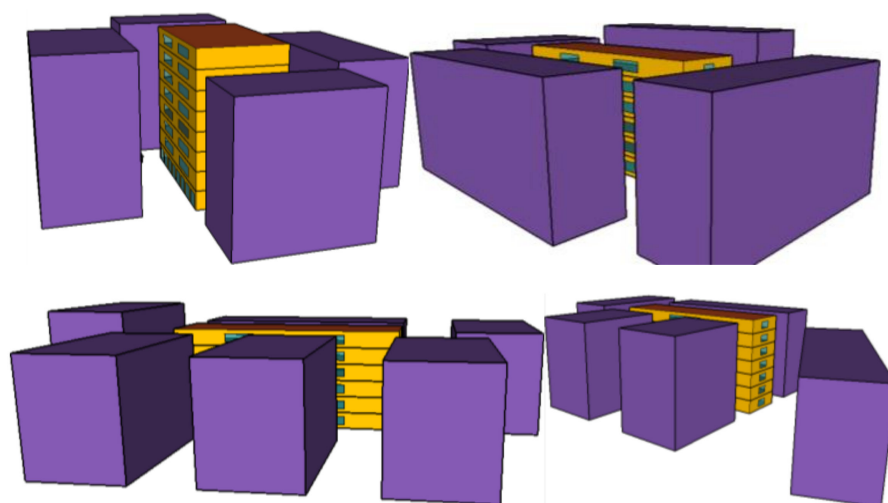**Figure 3.** Crowded residential district.

Figure 4. Building shading.

Table 5 summarizes the main electrical devices installed in the buildings, as well as the related power and heat gains, which are taken from [26,37]. The demand for domestic hot water is evaluated according to the Italian regulation UNI TS 11300 [38].

Table 5. The heat gain features of the appliances and devices [26,37].

Devices	Average Power (kW)	Heat Gain (kW)	Radiative Part (%)	Convective Part (%)
Fridge	0.040 (Naples) 0.060 (Fayoum)	0.040 (Naples) 0.060 (Fayoum)	0	100
Dishwasher	1.820	0.364	51	34
Bakery	0.870	0.522	14	49
Cooking plane	1.500	0.900	24	16
TV	0.240	0.240	40	60
PC (Processor: 3.5 GHz, RAM: 16 GB)	0.090	0.090	10	90
Laptop	0.059	0.059	25	75
Washing machine	1270 (Naples) 500 (Fayoum)	0.254 (Naples) 0.100 (Fayoum)	40	60

The same structure of the buildings is considered for the Fayoum district, where families, old people and young people account for 40%, 40% and 20% of the total population, respectively. Table 3 also shows that there are 9 buildings for families, 2 for old people and 2 for young people for Type A; 9 buildings for families, 3 for old people and 2 for young people for Type B; 9 buildings for families and 2 for old people for Type C and 8 buildings for families and 2 for old people for Type D. Note that Table 4 also summarizes the building envelope features located in the Fayoum district, which is characterized by a poor thermal insulation due to mild weather.

Table 6 displays the heating and cooling temporal profiles of both locations, as well as the set point temperatures for space heating and cooling.

Table 6. Building simulation input data.

Building Geometric Features	A	B	C	D
Building height (m^2)	24	18	18	21
Building volume (m^3)	7056	6840	8316	7980
Building floor area (m^2)	336	380	461	680
Number of building floors (-)	8	6	6	7
Number of apartments per building floor (-)	4	4	5	4
Apartment area (m^2)	84	95	92	95
Glass area (m^2)	254.75	221.75	264.20	240.48
Seasonal heating and cooling (Naples 1034-degrees day)	Heating: T_{set} = 20 °C [39] 15 November–31 March Cooling: $T_{set,residential}$ = 27 °C & $T_{set,commercial}$ = 26 °C 1 May–30 September [39]			
Seasonal heating and cooling (Fayoum 1096-degrees day)	Heating: T_{set} = 24 °C [35] 15 November–15 March Cooling: $T_{set,residential}$ = 28 °C & $T_{set,commercial}$ = 28 °C 1 May–31 October [35]			
Occupancy schedule (Naples)	See Reference [35]			
Occupancy schedule (Fayoum)				
Power load per day (kW) (Naples)				
Power load per day (kW) (Fayoum)				
Infiltration rate of air (vol/h)	0.6			
Average daily demand of DH (m^3/day)	194.17			
Set point temperature of DHW (°C)	45			

The reference systems (RSs) for both locations consist of the district, which was described above, where the demand for space cooling is satisfied by electrical air-to-air heat pumps. The thermal energy required for providing domestic hot water and building space heating is attained by conventional boilers with a rated efficiency of 0.75 (see Table 7).

Two different systems are proposed in Table 7. The first system for Fayoum (PS1 F) consists of the RS, where the roofs and walls of the district building are painted with cool paints (see Tables 7 and 8) to decrease the building solar absorbance to 0.17. The second proposed system for Fayoum (PS2 F) is the same as the RS, except for air-to-air heat pumps employed for building space cooling and building space heating. The domestic hot water is supplied by the conventional boiler, as in the RS (see Table 7). The third proposed system for Fayoum (PS3 F) consists of the layout described in Figure 1 (see Section 2 System Layout), where the electrical air-to-air heat pumps are still used for heating and cooling of the space. A district heating domestic hot water network (DHDHW) (see Figure 1 and see Section 2 System Layout) matches the demand for DHW, and the district is also served by an ETC plant of 1700 m^2 (Figure 1 and Tables 1 and 7). A condensing boiler with a capacity of 4.61 MW$_{th}$ is included as a backup system. A PV plant of 9397 m^2 supplies renewable power to the district to meet a share of the electricity demand, including the power delivered to the auxiliary hydraulic systems. Since the adoption of variable speed pumps enhances the energy performance of thermal districts [21,22], each branch of the district employs two 80 m^3/h pumps with fixed speeds and one 80 m^3/h pump with variable speed equipped with an inverter. The third proposed system for the district of Naples (PS3 N; Figure 1 and Table 7) is the same as Fayoum.

Table 7. Input parameters for the reference and proposed systems. DHW: domestic hot water.

System	Electric Energy	Heating of Building Space	Cooling of Building Space	DHW	Envelope			
					U_{roof} (W/m^2 K)	$\rho_{s,roof}$ (–)	U_{window} (W/m^2 K)	$g_{rwindows}$ (–)
Proposed System 1 (Fayoum)	Grid supplied	boiler $\eta_B = 0.75$	air-to-air HP	boiler $\eta_B = 0.75$	0.305	0.83	1.01	0.305
					0.916	0.83	2.89	0.789
Proposed System 2 (Fayoum)	Grid supplied			boiler $\eta_B = 0.75$	0.916	0.4	2.89	0.789
Proposed System 3 (Fayoum)	PV plant (9397 m^2) + grid			ETC plant (1700 m^2) + 4600 kW$_{th}$ condensing boiler $\eta_{CB} = 0.95$	0.916	0.4	2.89	0.789
Proposed System 3 (Naples)	PV plant (9397 m^2) + grid			ETC plant (1700 m^2) + 4613 kW$_{th}$ condensing boiler $\eta_{CB} = 0.95$	0.916	0.4	2.89	0.789

Table 8. Thermal insulation [40] and cool pain [30] technical specifications and cost figures.

Thermal Insulation	Conductivity	Density	Thickness	Cost
	W/mK	kg/m^3	m	€/m^2
Polyurethane	22	43	0.03	26.51
			0.04	31.45
			0.05	34.13
			0.06	40.67
			0.07	44.48
Roof painting	$\rho_{s,roof}$ -	ε -	**Painting style** kg/m^2	**Cost** €/kg
Cool painting	0.83	0.90	0.500	5.816

5. Results and Discussion

5.1. Balance of Energy, Economics and Environment

The annual energy demand for the electricity, heating and cooling of the space of the two districts in Naples and Fayoum is summarized in Table 9, with the share of $E_{el,LOAD}$ (electricity demand only for electric appliances and lights), $E_{el,tot}$ (total electricity demand related to $E_{el,LOAD}$, as well as the power required by the HPs), $E_{th,heat}$ and $E_{th,cool}$ (heating and cooling demands) and $E_{th,DHW}$ (thermal energy demand for DHW). Due to the different climates, the heating demand is higher in the Naples district, and the cooling demand is much lower. The total annual primary energy consumption of the district in Naples reaches 17.3 GWh, with an annual operating cost of 1.51 M€, while the total primary energy consumption of the Fayoum district reaches 17.2 GWh, and the annual operating cost is only 0.41 M€ because of the lower electricity price. The consumption of natural gas and the CO_2 emissions are also reported.

Table 9. Estimated annual performance (energy, economical and environmental) of the reference system in the districts located in Naples (RS N) and Fayoum (RS F).

	$E_{el,LOAD}$ (GWh)	$E_{el,tot}$ (GWh)	$E_{th,heat}$ (GWh)	$E_{th,cool}$ (GWh)	$E_{th,DHW}$ (GWh)	PE (GWh)	C (M€)	Vol_{NG} (Sm^3)	CO_2 (Gg)
RS N	3.9	4.0	4.0	0.5	2.5	17.3	1.5	900,594	3.7
RS F	3.6	4.1	3.7	2.0	2.5	17.2	0.4	860,000	3.4

Three energy efficiency strategies were proposed: PS1, PS2 and PS3. The results, including the comparisons with the reference system (RS), are shown in Tables 10 and

11. For PS1, the primary energy consumption is slight lower than for the RS in the Naples district, while a slight decrease in the energy performance in the Fayoum district is observed. The reduction of the walls/roofs solar absorbance decreases the solar gain, so that a higher heating demand is found in the winter. The resulting payback period of PS1 in both districts is extremely high. PS2 achieves better energetic, environmental and economic performances for both districts. This is due to the high efficiency of the HPs proposed in PS2 compared to the efficiency of conventional condensing boilers. In particular, the primary energy savings, CO_2 emissions reduction and decrease in annual operating costs are 16.0%, 16.2% and 0.016 M€/year for the Fayoum district in the PS2 case in comparison to PS1, and similar results were obtained for Naples.

Table 10. Annual energetic results of the proposed systems for the districts located in Naples and Fayoum.

	$E_{el,tot}$ (GWh)	$E_{th,heat\&cool}$ (GWh)	*PE* (GWh)	ΔPE (GWh)	*PES* (%)	ΔCO_2 (Gg)	ΔCO_2 (%)
PS1 N	4.0	4.0	16.8	0.5	2.8	0.01	2.7
PS2 N	5.1	4.5	14.4	2.9	16.9	0.5	14.7
PS3 N	5.1	4.5	7.3	10.1	58.2	2.1	56.8
PS1 F	3.9	5.5	17.8	−0.7	−3.8	−0.1	−3.8
PS2 F	5.1	5.7	14.4	2.7	16.0	0.6	16.2
PS3 F	5.1	5.7	5.7	11.4	66.7	2.3	66.8

Table 11. Annual economic results of the proposed systems for the districts located in Naples and Fayoum.

	C (M€/Year)	ΔC (M€/Year)	*SPB* (Year)	*PI* (-)	*NPV* (M€)	C_{inv} (M€)	ΔVol_{NG} (Sm^3)
PS1 N	1.47	0.04	71	−0.80	−2.52	3.14	42,600
PS2 N	1.22	0.29	0	-	4.38	0	557,000
PS3 N	0.63	0.88	5	1.75	6.82	3.89	769,000
PS1 F	0.41	0.003	182	−0.92	−0.51	0.56	118,000
PS2 F	0.43	0.016	0	-	-	0	515,000
PS3 F	0.25	0.167	23	−0.39	−1.53	3.89	754,000

PS3 considers PV panels to generate electric energy and ETCs to obtain thermal energy from solar radiation. It can be observed from Table 11 that the primary energy saving in comparison to PS1 reaches 58.2% and 66.6% for the Naples district and the Fayoum district, and the reduction of CO_2 emissions is 56.8% and 66.8%. From the economic perspective, PS3 requires an annual operating cost of 0.63 M€, and it offers an economic savings of 0.88 M€ per year in the Naples district, while, in the Fayoum district, the operating cost is 0.25 M€, and the economic savings are 0.167 M€. In the case of Fayoum, although the payback period of this renewable energy system is significantly lower than the payback period of PS1, the period of 23 years still indicates that this strategy is not profitable at the current stage as a result of the lower electricity and natural gas prices in Fayoum. However, with the increase of energy prices and the growing attention for sustainability, such systems could increase their profitability. For the Naples district, the payback period of PS3 is five years, which indicates a promising potential in real applications.

The details of the energy performance analysis of PS3 are listed in Table 12, which highlights the influence of the renewable energy assets. PV panels are able to generate 3.1 GWhe per year in the Fayoum district, of which 58% is self-consumed, and it covers nearly 35% of the total electricity demand. The thermal energy produced by the ETCs is 1.1 GWh per year in Naples, covering 47% of the total energy required for DHW, and it is 1.6 GWh per year in the Naples district, with a coverage 62% of the DHW demand. This is due to the higher solar irradiance of Fayoum in comparison to Naples. On the other side, Fayoum has a significantly higher annual cooling demand than Naples.

Table 12. Annual results of the renewable system (PS3) for the districts located in Naples and Fayoum.

	$E_{el,PV}$ (GWh)	$E_{th,ETC}$ (GWh)	$E_{el,toGRID}$ (GWh)	$E_{el,self}$ (GWh)	$E_{el,self}/E_{el,tot}$ (%)	$E_{el,self}/E_{el,PV}$ (%)	η_{PV} (-)	η_{ETC} (-)	R_{ETC} (%)	R_{CB} (%)
PS3 N	2.5	1.1	0.9	1.5	28.8	59.0	0.15	0.36	46.79	53.2
PS3 F	3.1	1.6	1.2	1.8	35.3	57.9	0.15	0.41	61.71	39.0

Concerning the renewable district proposed for the Naples district, the generated power by the PV plant satisfies about 29% of the district's electricity demand, of which 59% is self-consumed. The solar thermal energy provides 62% of the thermal energy demand for DHW, as seen from Table 12.

5.2. Energy Demand and Generation Profiles

Temporal profiles of the energy demand of the RS, including the demand for heating, cooling and electricity, for representative summer and winter days are depicted in Figures 5 and 6, respectively. Note that, in both graphs, the ambient temperature is also included to indicate its effect on the thermal energy for the heating and cooling of the space. Figure 6a displays that the demand for heating (Q_{heat}) of the Naples district reaches the peak value of 9770 kW$_{th}$ at 12:30, as the heating systems are turned on in the majority of the apartments.

(a)

(b)
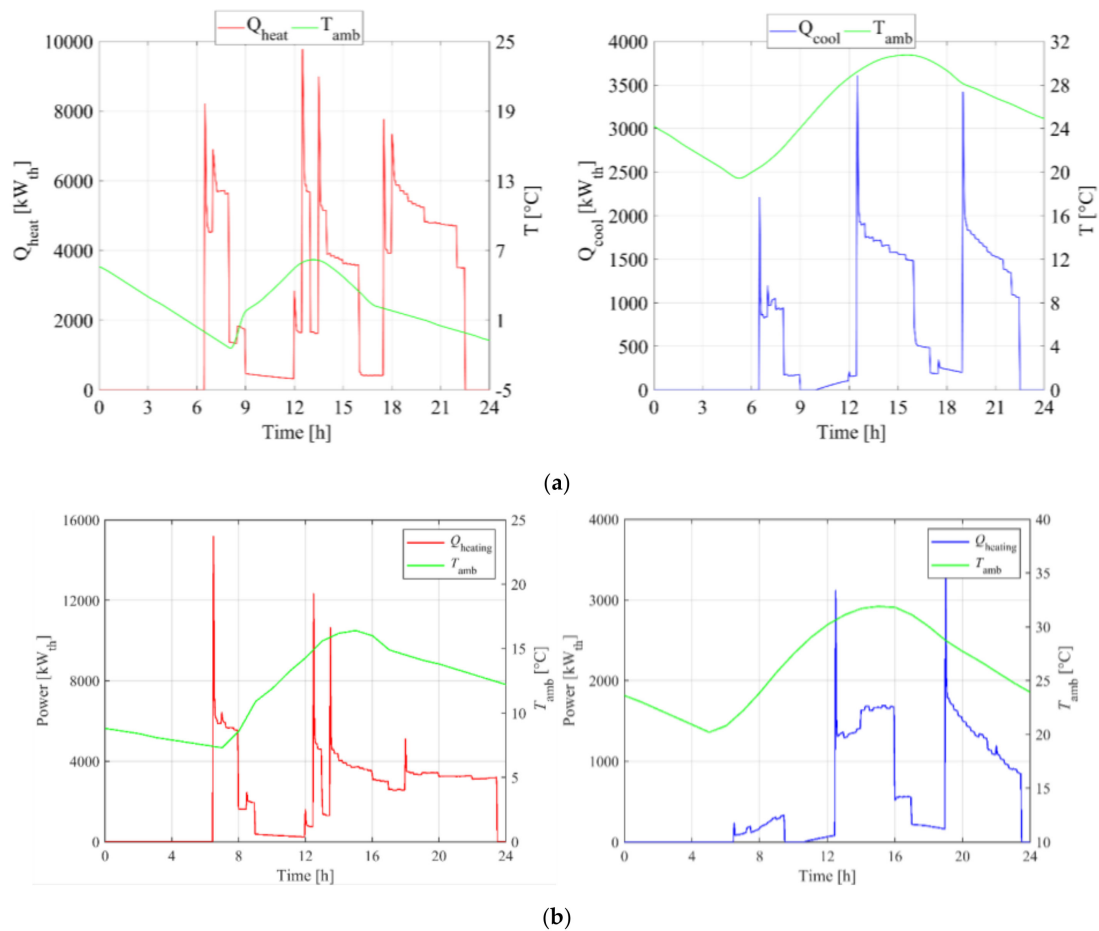
Figure 5. Thermal energy demand profile for a representative winter day (left) and a representative summer day (right) of the districts located in (**a**) Naples and (**b**) Fayoum.

(**a**)

(**b**)
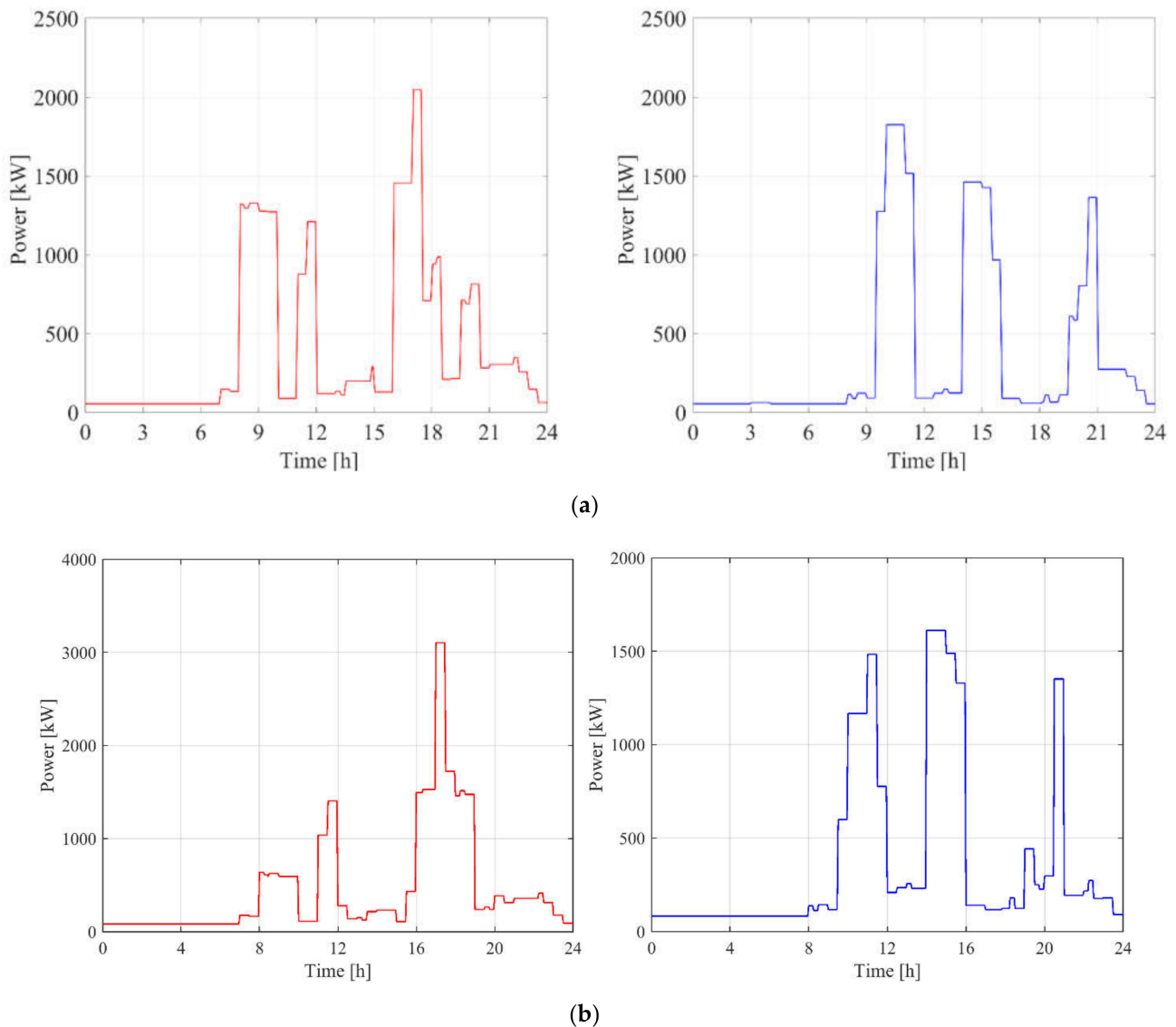
Figure 6. Thermal energy demand profile for a representative winter day (left) and a representative summer day (right) of the districts located in (**a**) Naples and (**b**) Fayoum.

Note that the space heating demand is remarkably higher than that for space cooling (Q_{cool}). This result is mainly related with the shading that the buildings make for each other. For the district in Fayoum (see Figure 6b), the heating demand occurs from 06:00 to 23:30 for a winter day, which is contributed both by the apartments and commercial zones, and it mainly occurs over two small time ranges, i.e., 06:30–09:00 and 12:00–23:30. The heating demand reaches the maximum value of 15.2 kW$_{th}$ at about 6:30 in the morning, when the heating systems are turned on in most of the apartments. On the other side, the demand for cooling in the summer day mainly occurs during 12:30–17:00 and 19:00–23:30, with the maximum of 3300 kW$_{th}$ obtained at 19:00. As the ambient temperature is also lower than the indoor temperature—in particular, in the early morning and night—the cooling demand decreases. The obtained results further confirm that the total heating demand exceeds the total cooling demand (see Figure 5). The influence of both the incident radiation and internal thermal energy gains from electrical devices on the demand for heating and cooling is also included in the proposed model. The incident radiation is affected by the shade resulting from the buildings of the district on each other, which increases the space heating demand in the winter while reducing the space cooling demand in the summer.

Although the internal thermal energy gains from the electrical devices due to appliances and lights have a benefit on the heating demand, it negatively affects the cooling demand.

The electric load is mainly related to the apartment occupation schedule and the operation strategy of the electrical devices, which are affected by the living habits of the residents in the specific districts. Figure 7 shows the electric load on the same winter and summer days as Figure 6. The maximum electric load of 2047 kW is detected at 17:00 in the Naples district, while on the summer day, the maximum electric load of 1825 kW is obtained at 10:05 (Figure 6). The peak of the power consumption of 3100 kW is achieved at 17:00 on the winter day in the Fayoum district, while the maximum power consumption on the summer day is obtained at 14:00, equal to 1610 kW.

(a)

(b)
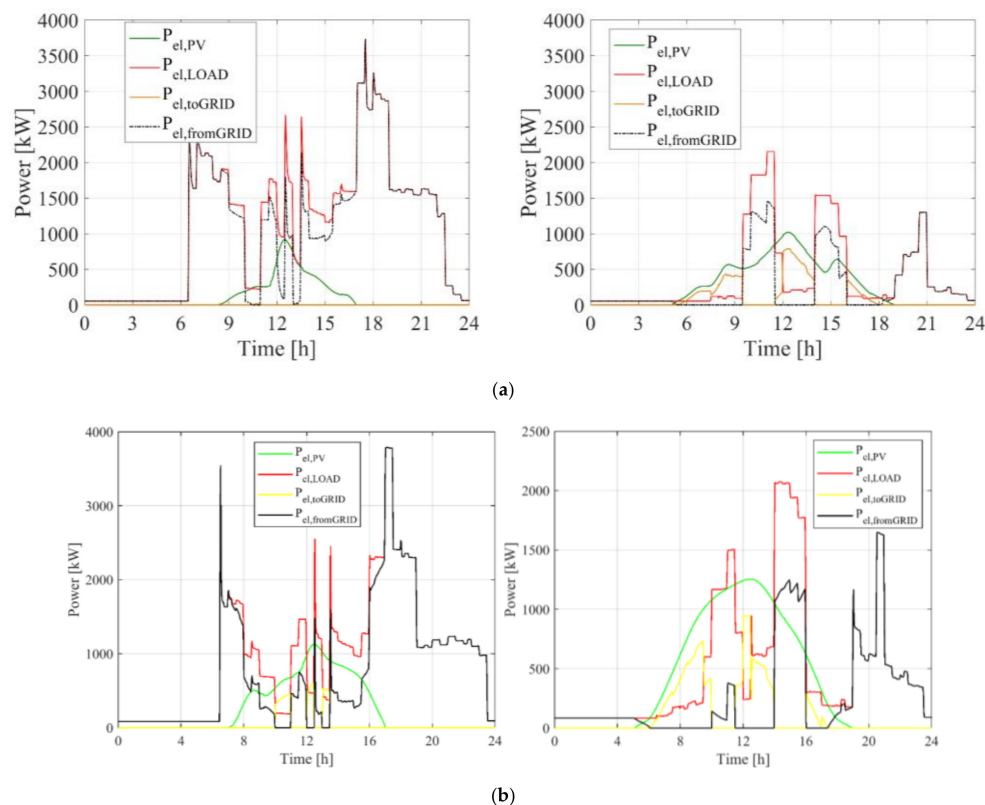
Figure 7. Dynamic results on a representative winter day (left) and a representative summer day (right) of the proposed system 3 (PS3) for the districts located in (**a**) Naples and (**b**) Fayoum.

The temporal profile of PV generation, as well as the amount of power withdrawn from and delivered to the grid are shown in Figure 7. On the winter day, PV panels are able to generate power from 07:30 to 16:30 when solar energy is available, with a peak value of 1100 kW at around 12:10. Since the power generated by the PV panels is considerably lower than the total demand, the district is still dependent on the grid. While on the summer day, with the higher solar irradiance, PV panels are able to cover a substantial fraction of the total electricity demand, and the peak power output by the PV panels reaches 1250 kW. It can also be observed that the reference system and the proposed system PS 3 for the district of Fayoum exhibit similar trends relative to the Naples district, of which more detailed information is available in Reference [35].

5.3. Monthly Results

The monthly results of the PS3 are analyzed in this section. Figure 8 shows the energy demand for the heating, cooling and electricity of both districts. January is featured by the highest thermal energy demand, equal to 1060 MWh for the Naples district and 1200 MWh for the Fayoum district (Figure 8). The highest demand for space cooling is obtained in July

in the Naples district: $E_{th,cool}$ equal to 210 MWh, while the cooling demand in the Fayoum district is much higher, which reaches 510 MWh (Figure 8). It can also be observed that the required thermal energy for heating $E_{th,heat}$ is obviously higher than that for cooling $E_{th,cool}$, which further confirms the dynamic results above (see Figure 5).
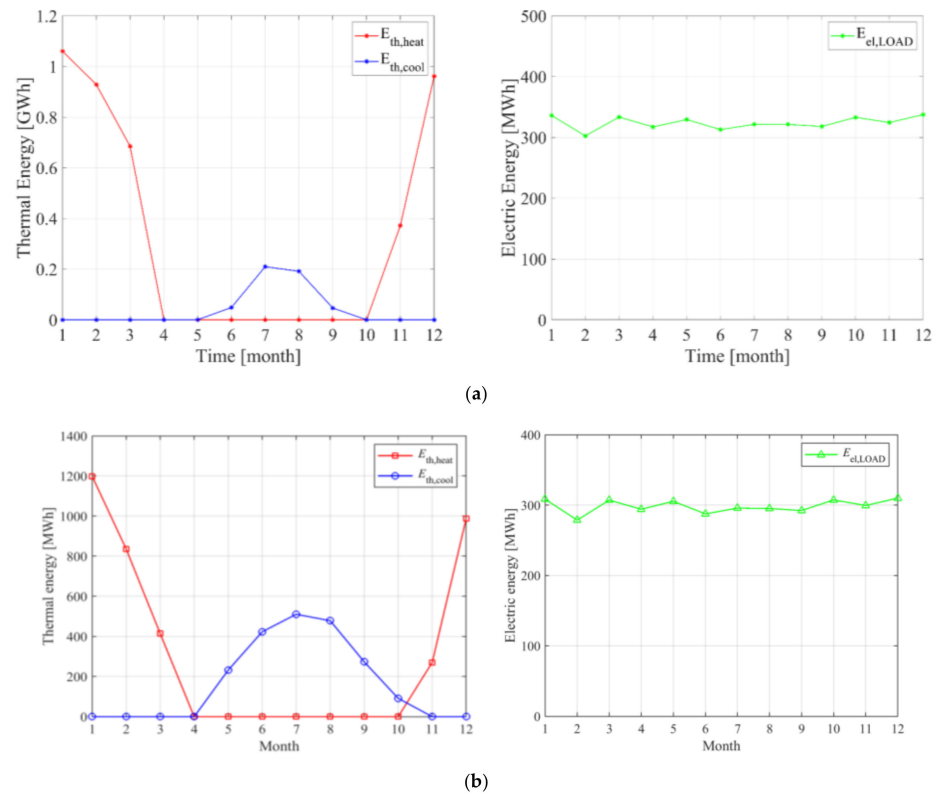

Figure 8. Monthly demands of the thermal and electric energies of the districts located in (**a**) Naples and (**b**) Fayoum.

The amounts of electricity generated, self-consumed, sold/injected to the grid and imported/bought from the grid are shown in Figure 9. For the Naples district, the grid meets a larger share of the electricity demand, and the ratio "$E_{el,fromGRID}/E_{el,LOAD}$" is constantly higher than 53% over months. The highest fraction of self-consumed electricity is 47%, and it is realized in June. The electricity generated from the PV plant is able to satisfy 46% of the demand for electricity over all the months. For the Fayoum district, the PV panels can satisfy over 33% of the total electricity demand over all the months, and the maximum fraction reaches nearly 50%. A large amount of electricity needs to be bought/imported from the grid, and hence, the district is still dependent on the grid, as was specified above. The highest fraction of self-consumed electricity is obtained in July, which reaches 32%. It can be noted that more than 39% of the electricity generated by the PV panels is self-consumed, and the maximum value achieved reaches nearly 67% in both July and August. The ratio of "$E_{el,PV}/E_{el,LOAD}$" is constantly higher than "$E_{el,self}/E_{el,LOAD}$", indicating that the electricity generation and demand are not synchronous, and hence, part of the electricity generated by the PV panels is injected into the grid, and this opens opportunities for electric storage to minimize the electricity exchange with the grid (Figure 9).
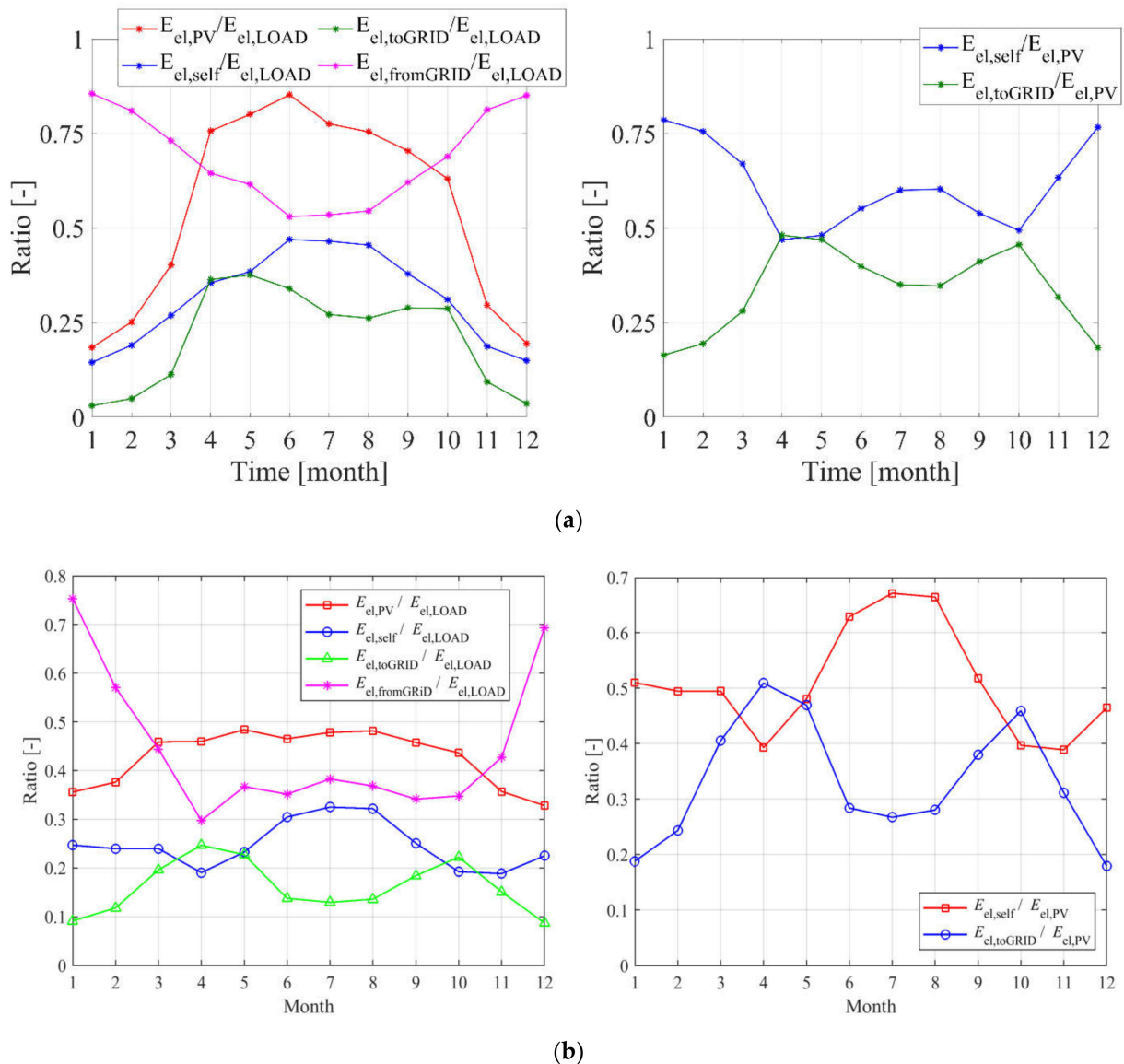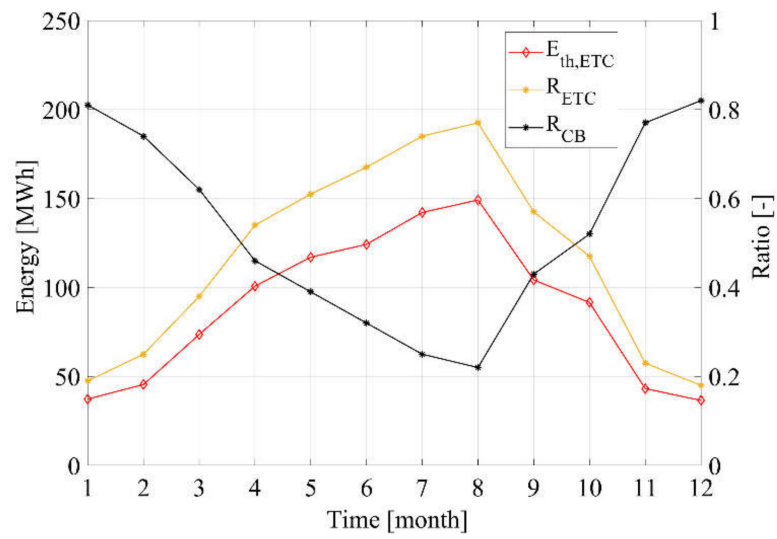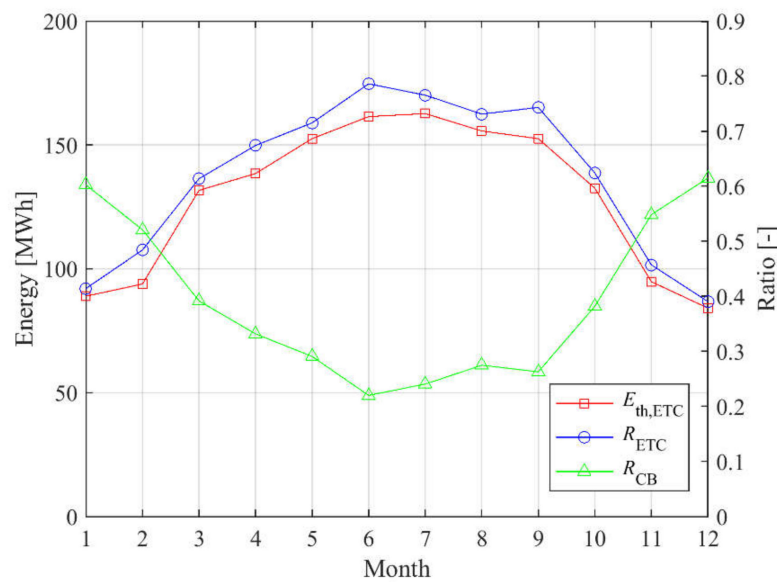
Figure 9. Monthly results of the energy ratios of the electric energy demand and energy ratios of the produced photovoltaic (PV) electric energy of the third proposed system (PS3) for the districts located in (**a**) Naples and (**b**) Fayoum.

Figure 10 shows the monthly results of the ETC plant, which plots the generated thermal energy by the plant ($E_{th,ETC}$), the ratio of the thermal energy supplied by ETC to the thermal energy demand for DHW (R_{ETC}) and the ratio of the thermal energy provided by the auxiliary natural gas-based condensing boiler to the thermal energy demand for DHW (R_{CB}). It can be seen that $E_{th,ETC}$ correlates with the solar radiation, and hence, it is higher during the summer, with a maximum capacity of 149 MWh for the Naples district and 162 MWh for the Fayoum district in July. The ETC plant is able to cover 54–77% (Naples) and 67–79% (Fayoum) of the thermal energy required by DHW (from April to September), while the condensing boilers provide a high amount of thermal energy in the remaining period (Figure 10).

(a)

(b)

Figure 10. Monthly results: energy performance of the ETC of the PS3 for the scenario of (**a**) Naples and (**b**) Fayoum.

Figures 11 and 12 display the ratios evaluated as follows:

$$R_{heat} = \frac{E_{th,heat,Naples} - E_{th,heatFayoum}}{E_{th,heat,Naples}}$$
$$R_{cool} = \frac{E_{th,cool,Naples} - E_{th,cool,Fayoum}}{E_{th,cool,Naples}} \qquad (10)$$
$$\text{Re}l = \frac{E_{el,Naples} - E_{el,Fayoum}}{E_{el,Naples}}$$
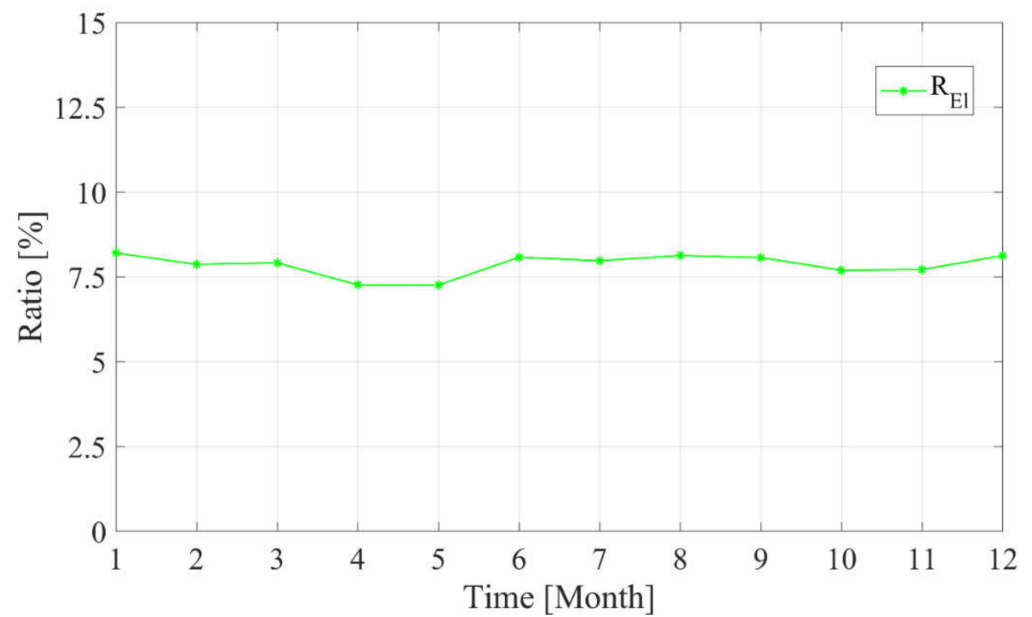
Figure 11. Monthly electric energy differences.
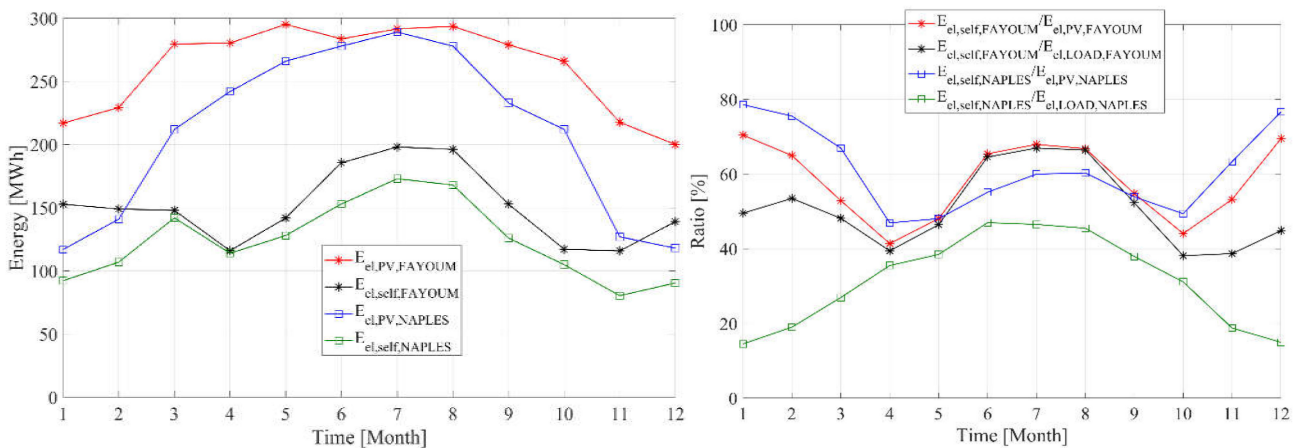
Figure 12. Renewable layout differences between Fayoum and Naples.

Note that the cooling energy ratios were evaluated only for the months in which the cooling energy demand exists both in the Fayoum and Naples district. It can be noted from Figure 13 that the heating energy demand in Naples is higher than that in Fayoum during most of the heating season, and the maximum deviation reaches 40% in March. Conversely, the heating energy demand in January in Fayoum is higher than the one in Naples. This is related to the poor thermal insulation of the buildings located in Fayoum (see Table 4). For the cooling demand, the district in Naples requires a significantly lower amount than that of Fayoum in the cooling season, which is related to the hot climate conditions in Egypt. The differences in electric energy demands in the two districts keep steady throughout the year, which is approximately 7.5% in all the months as proven by Figure 11.
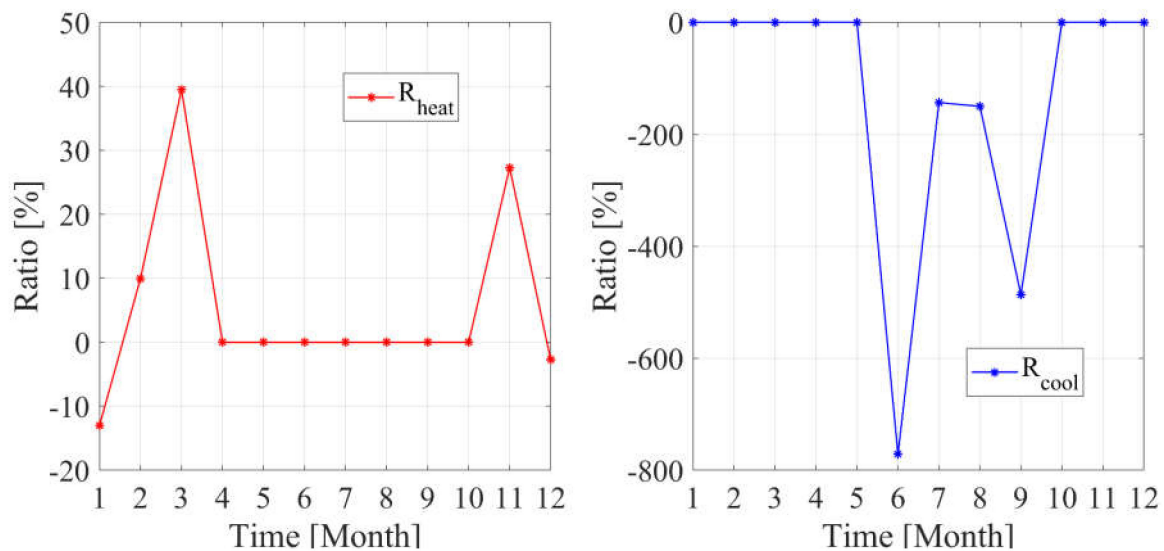
Figure 13. Monthly thermal energy differences.

Figure 12 shows the differences between the results of the renewable energy systems in the two districts (PS3). The PV plant generates a higher electric energy in Fayoum than that in Naples, thanks to the higher solar irradiance, while in the summer, the two renewable systems yield similar performances. As a consequence, the $E_{el,self}$ of the district in Fayoum is also higher, which indicates that the electricity supplied by the PV plant is able to meet the total demand for electricity in the Fayoum district. Similarly, the $E_{el,self}/E_{el,LOAD}$ of the district in Fayoum is also higher than that in Naples, which further confirms that the PV plant plays a more significant role in the Fayoum district. While the comparison of the ratio of $E_{el,self}/E_{el,PV}$ indicates that more electricity generated by the PV plant is self-consumed in the summer in the Fayoum district, the ratio is higher in the Naples district during the other times throughout the year.

6. Conclusions

This work proposes a techno-economic assessment of different energy efficiency measures implemented in two districts in Fayoum and Naples.

Three innovative energy measures were modeled and simulated in TRNSYS in order to quantify and analyze the primary energy savings. The renewable district involved a district heating network for s domestic hot water feed by a solar-evacuated collector plant. In addition, the electricity demand of the district, including electricity required by the appliances in each apartment and electricity for air-to-air heat pumps, was met by a photovoltaic plant.

The main findings are summarized as follows:

- The residential district of Fayoum features a yearly thermal energy demand of 3.7 GWh for heating and 2.0 GWh for cooling. The cooling demand of the investigated district in Fayoum is significantly higher than the cooling demand of the district located in Naples, i.e., 0.5 GWh, due to the higher solar irradiance in Fayoum. Conversely, the heating energy demand of the Naples district is almost similar to the one of Fayoum, being equal to 4.0 GWh.
- The district located in Fayoum has an annual demand of primary energy of 17 GWh, with an annual operating cost of 0.41 M€/year.
- The envelope refurbishment for the district located in Fayoum, dealing with the use of cool paint for the roof, led to a very long payback period. This is mainly due to the low electricity price in Egypt.
- The adoption of electric-driven air-to-air heat pumps reduced the consumption of primary energy. In particular, the consumption of primary energy of the district

located in Fayoum decreased by 16% due to the high efficiency of the heat pumps compared to the efficiency of the condensing boilers.

- The renewable energy measure based on photovoltaic panels, evacuated solar collectors and air-to-air heat pumps reached a promising primary energy savings of 67% in the Fayoum district and 58% in the Naples district. The differences were mainly related to the higher solar radiation in Fayoum with respect to Naples. These results suggest that this solution is quite promising in reducing the consumption of primary energy and the environmental impact of residential districts located in the Mediterranean region.

- The payback period of the renewable energy system in Naples is five years, while, in Fayoum, is 23 years, which shows that this energy-efficient renovation is not profitable, as expected. This is mainly related to the lower electricity and natural gas prices in Fayoum. However, with the increase of energy prices and the growing attention for environment protection, such systems could offer interesting profitability.

In conclusion, the proposed renewable district based on a domestic hot water network fed by an ETC plant and a PV plant represents a suitable and very promising energy measure to decarbonize residential districts. As a matter of fact, air-to-air heat pumps coupled with photovoltaic panels are able to significantly reduce the primary energy consumptions for buildings' space heating and cooling. In addition, the use of air-to-air heat pumps, fed by an electrical grid, is also able to limit the primary energy consumption for buildings' space heating and cooling due to the higher efficiency when compared to gas-fired boilers. Therefore, this technology may be easily and quickly adopted by districts, especially with a Mediterranean climate, where the performances of heat pumps are especially high.

Future developments of this work may involve electric storage assets to better address the mismatch of power production and demand.

Abbreviations

A	area (m^2)
c	cost-price per unit (€/kWh or €/m^2 or €/m or €/t)
c_p	specific heat at constant pressure (kJ kg^{-1} K^{-1})
G	incident solar total radiation (W m^{-2})
C_{inv}	capital cost for a component/system (€)
k	counter (-)
LHV	lower heating value (kWh Sm^{-3})
$\dot{m}$	mass flow rate (kg s^{-1})
m_{PV}	Percent of annual PV maintenance (%/year)
m_{ETC}	Percent of annual ETC maintenance (%/year)
N_p	number of people (-)
N_{par}	number of PV modules in parallel (-)
N_s	number of PV modules in series (-)
NPV	net present value (€)

P	electric power (kW)
PE	primary energy (kWh/year)
PES	primary energy saving (-)
PI	profit index
$\dot{Q}$	thermal power (kW)
SPB	simple pay back (years)
T	temperature (°C)
U	overall heat transfer coefficient (W m^{-2} K^{-1})
v	velocity (m s^{-1})
Vol	volume (m^3)
Greek Symbols	
Δ	difference (-)
ε	long wave *emissivity* (-)
η	efficiency (-)
ρ	density (kg m^{-3})
ρ$_s$	solar reflectance *(-)*
Subscripts	
amb	ambient
act	activation
avg	average
B	referred to boiler
CB	referred to condensing boiler
conv	convective
cool	cooling
DHW	domestic hot water
E	energy
el	electric
ETC	evacuated solar thermal collector
from GRID	electric energy imported from national power grid
indoor	indoor electric load
LOAD	electric demand
min	minimum
NG	natural gas
out	output
p	primary energy
PS	proposed system
PV	photovoltaic plant
RS	reference system
self	self-consumed electric energy
solar	thermal solar energy
t	value of a parameter in time step t
th	thermal
to GRID	electric energy sent to national electric grid
Tk	tank
u	user

References

1. International Energy Agency—IEA. *Energy Climate and Change—World Energy Outlook Special Report*; Special Report on Energy and Climate Change; IEA: Paris, France, 2015.
2. Lake, A.; Rezaie, B.; Beyerlein, S. Review of district heating and cooling systems for a sustainable future. *Renew. Sustain. Energy Rev.* **2017**, *67*, 417–425. [CrossRef]
3. Lund, H.; Werner, S.; Wiltshire, R.; Svendsen, S.; Thorsen, J.; Hvelplund, F.; Vad Mathiesen, B. 4th Generation District Heating (4GDH): Integrating smart thermal grids into future sustainable energy systems. *Energy* **2014**, *68*, 1–11. [CrossRef]
4. Carpaneto, E.; Lazzeroni, P.; Repetto, M. Optimal integration of solar energy in a district heating network. *Renew. Energy* **2015**, *75*, 714–721. [CrossRef]
5. Calise, F.; Cappiello, F.L.; D'Accadia, M.D.; Vicidomini, M. Thermo-Economic Analysis of Hybrid Solar-Geothermal Polygeneration Plants in Different Configurations. *Energies* **2020**, *13*, 2391. [CrossRef]

6. Alkan, A.M.; Keçebaş, A.; Yamankaradeniz, N. Exergoeconomic analysis of a district heating system for geothermal energy using specific exergy cost method. *Energy* **2013**, *60*, 426–434. [CrossRef]
7. Unternährer, J.; Moret, S.; Joost, S.; Maréchal, F. Spatial clustering for district heating integration in urban energy systems: Application to geothermal energy. *Appl. Energy* **2017**, *190*, 749–763. [CrossRef]
8. Fang, H.; Xia, J.; Zhu, K.; Su, Y.; Jiang, Y. Industrial waste heat utilization for low temperature district heating. *Energy Policy* **2013**, *62*, 236–246. [CrossRef]
9. Fang, H.; Xia, J.; Jiang, Y. Key issues and solutions in a district heating system using low-grade industrial waste heat. *Energy* **2015**, *86*, 589–602. [CrossRef]
10. Aunedi, M.; Pantaleo, A.M.; Kuriyan, K.; Strbac, G.; Shah, N. Modelling of national and local interactions between heat and electricity networks in low-carbon energy systems. *Appl. Energy* **2020**, *276*, 115522. [CrossRef]
11. Gabrielli, P.; Gazzani, M.; Martelli, E.; Mazzotti, M. Optimal design of multi-energy systems with seasonal storage. *Appl. Energy* **2018**, *219*, 408–424. [CrossRef]
12. Mateu-Royo, C.; Sawalha, S.; Mota-Babiloni, A.; Navarro-Esbrí, J. High temperature heat pump integration into district heating network. *Energy Convers. Manag.* **2020**, *210*, 112719. [CrossRef]
13. Roselli, C.; Sasso, M.; Tariello, F. Integration between electric heat pump and PV system to increase self-consumption of an office application. Renew. *Energy Environ. Sustain.* **2017**, *2*, 28. [CrossRef]
14. Roselli, C.; Sasso, M.; Tariello, F. Dynamic Simulation of a Solar Electric Driven Heat Pump for an Office Building Located in Southern Italy. *Int. J. Heat Technol.* **2016**, *34*, S496–S504. [CrossRef]
15. Izquierdo, M.; de Agustín, P.; Martín, E. A Micro Photovoltaic-heat Pump System for House Heating by Radiant Floor: Some Experimental Results. *Energy Procedia* **2014**, *48*, 865–875. [CrossRef]
16. Dai, B.; Qi, H.; Liu, S.; Zhong, Z.; Li, H.; Song, M.; Ma, M.; Sun, Z. Environmental and economical analyses of transcritical CO_2 heat pump combined with direct dedicated mechanical subcooling (DMS) for space heating in China. *Energy Convers. Manag.* **2019**, *198*, 111317. [CrossRef]
17. Calabrese, N.; Mastrullo, R.; Mauro, A.W.; Rovella, P.; Tammaro, M. Performance analysis of a rooftop, air-to-air heat pump working with CO_2. *Appl. Thermal Eng.* **2015**, *75*, 1046–1054. [CrossRef]
18. Heibati, S.; Maref, W.; Saber, H.H. Assessing the Energy and Indoor Air Quality Performance for a Three-Story Building Using an Integrated Model, Part One: The Need for Integration. *Energies* **2019**, *12*, 4775. [CrossRef]
19. Li, H.; Xu, W.; Yu, Z.; Wu, J.; Yu, Z. Discussion of a combined solar thermal and ground source heat pump system operation strategy for office heating. *Energy Build.* **2018**, *162*, 42–53. [CrossRef]
20. Paiho, S.; Ketomäki, J.; Kannari, L.; Häkkinen, T.; Shemeikka, J. A new procedure for assessing the energy-efficient refurbishment of buildings on district scale. *Sustain. Cities Soc.* **2019**, *46*, 101454. [CrossRef]
21. Gong, E.; Wang, N.; You, S.; Wang, Y.; Zhang, H.; Wei, S. Optimal operation of novel hybrid district heating system driven by central and distributed variable speed pumps. *Energy Convers. Manag.* **2019**, *196*, 211–226. [CrossRef]
22. Gu, J.; Wang, J.; Qi, C.; Yu, X.; Sundén, B. Analysis of a hybrid control scheme in the district heating system with distributed variable speed pumps. *Sustain. Cities Soc.* **2019**, *48*, 101591. [CrossRef]
23. Calise, F. Thermoeconomic analysis and optimization of high efficiency solar heating and cooling systems for different Italian school buildings and climates. *Energy Build.* **2010**, *42*, 992–1003. [CrossRef]
24. Klein, S.A.; Beckman, W.; Mitchell, J.W.; Duffie, J.A.; Duffie, N.A.; Freeman, T.L. *Solar Energy Laboratory, TRNSYS. A Transient System Simulation Program*; Solar Energy Laboratory, University of Wisconsin: Madison, WI, USA, 2006.
25. Buonomano, A.; Calise, F.; Palombo, A.; Vicidomini, M. BIPVT systems for residential applications: An energy and economic analysis for European climates. *Appl. Energy* **2016**, *184*, 1411–1431. [CrossRef]
26. American Society of Heating, Refrigerating and Air-Conditioning Engineers. *ASHRAE Handbook: Fundamentals*; ASHRAE: Atlanta, GA, USA, 1993.
27. Murray, M.C.; Finlayson, N.; Kummert, M.; Macbeth, J. Live Energy Trnsys -Trnsys Simulation within Google Sketchup. In Proceedings of the Eleventh International IBPSA Conference, Glasgow, Scotland, 27–30 July 2009.
28. Piemonte, R. Bollettino Unico Regione Piemonte. 2018. Available online: http://www.regione.piemonte.it/oopp/prezzario/dwd/2018/Prezzario_Regione_Piemonte_2018.pdf (accessed on 1 July 2020).
29. Government of Egypt. Available online: https://www.egas.com.eg/ (accessed on 1 July 2020).
30. ISOVER. 2019. Available online: http://bituver.it/impermeabilizzazione/prodotti/gamma-ad-alta-riflettanza/california-p/ (accessed on 1 July 2020).
31. Buonomano, A.; Calise, F.; d'Accadia, M.D.; Vicidomini, M. A hybrid renewable system based on wind and solar energy coupled with an electrical storage: Dynamic simulation and economic assessment. *Energy* **2018**, *155*, 174–189. [CrossRef]
32. Buonomano, A.; Calise, F.; Palombo, A.; Vicidomini, M. Adsorption chiller operation by recovering low-temperature heat from building integrated photovoltaic thermal collectors: Modelling and simulation. *Energy Convers. Manag.* **2017**, *149*, 1019–1036. [CrossRef]
33. Calise, F.; Cappiello, F.L.; Dentice d'Accadia, M.; Vicidomini, M. Dynamic simulation, energy and economic comparison between BIPV and BIPVT collectors coupled with micro-wind turbines. *Energy* **2020**, *191*, 116439. [CrossRef]
34. SALMSON. 2019. Available online: http://www.salmson.com/index.php?id=19&L=2 (accessed on 15 September 2020).

35. Ministry of Housing, Egypt. Energy Efficiency Commercial Building Code. Available online: http://www.hbrc.edu.eg/code.html (accessed on 18 December 2020).

36. Luca, A.P.G.D.; Patto dei Sindaci. *Piano di Azione per L'energia Sostenibile (PAES)—Relazione Specialistica Sull'efficienza Energetica negli Edifici (Climatizzazione e Acqua Calda Sanitaria)*; Patto dei Sindaci: Napoli, Italy, 2018.

37. Agenzia nazionale per le nuove tecnologie2019. Available online: http://www.enea.it/it (accessed on 10 May 2020).

38. Specifica Tecnica UNI TS 11300-2:2019. UNI TS 11300. 2019. Available online: https://www.certifico.com/aziende-safety/234-consulting/norme-tecniche/index.php?option=com_content&view=article&id=7781&catid=358&Itemid=494 (accessed on 10 May 2020).

39. Calise, F.; Cappiello, F.L.; D'Accadia, M.D.; Vicidomini, M. Energy efficiency in small districts: Dynamic simulation and technoeconomic analysis. *Energy Convers. Manag.* **2020**, *220*, 113022. [CrossRef]

40. Alimonti, C.; Conti, P.; Soldo, E. A comprehensive exergy evaluation of a deep borehole heat exchanger coupled with a ORC plant: The case study of Campi Flegrei. *Energy* **2019**, *189*, 116100.